Effect of tissue inhomogeneity on electric field intensity for electrochemotherapy treatment

Elisabetta Sieni[1], Paolo Sgarbossa[1], Fabrizio Dughiero[1], Michele Forzan[1], Paolo Di Barba[2], Maria Evelina Mognaschi[2], Tejasvi Parupudi[3], Lakshya Mittal[4], Ignacio G. Camarillo[5,6], and Raji Sundararajan[4]

[1]Industrial Engineering Dept. Padova University, Italy
[2]Pavia University, Italy
[3]Electrical & Computer Engineering Dept., Purdue University, IN 47907
[4]School of Engineering Technology, Purdue University, IN 47907
[5]Biological Sciences Dept., Purdue University, IN 47907
[6]Center for Cancer Research, Purdue University, IN 47907
e-mail: raji@purdue.edu

Abstract—Presented in this paper is a useful model to evaluate the effect of tissue inhomogeneity in terms of electric field distribution when electroporation is applied to permeabilize cells for enhanced uptake of chemodrugs. The electric field is evaluated by means of Finite Element Analysis and is compared with the distribution found in a phantom model. The phantoms are built using potato that becomes dark if electroporated, and a Tissue-Mimic-Material, where the resistivity can be suitably designed. For this purpose, a pair of needles, with 2 cm gap was used to apply electric field. Both the numerical model and the phantom include a parallelepiped of homogeneous material with needles and a hole with diameter 7 mm, filled with materials with different resistivities. The hole in the middle, between the needles, simulates the inhomogeneity. This model can show the variation in the electric field when tissue inhomogeneities occur. The results illustrate the variations in the electric fields at different regions, which has promising clinical practice.

I. Introduction

Electrochemotherapy, an emerging technique, for treating cancers involves applying high intensity, short duration pulses to enhance the drug uptake through the normally impermeable or less permeable cell membranes [1–3]. Electric field intensity and distribution is critical to open up pores and enhance the drug uptake. Typically, 4mm or 7 mm gap electrodes are used to treat the tumors [4–6]. Hence, it requires multiple applications for treating larger areas; thus, extended time of operation and sedation to the patient [7]. To alleviate this, a large grid electrode has been designed and developed [7–9]. However, since a larger area is covered by the grid electrode, there is tissue inhomogeneity to be taken into account for the application of electrochemotherapy on large areas, like, chest wall carcinoma after mastectomy [10,11]. Due to scars and breast tissue, the

remaining surface could show tissue inhomogeneity, since different tissues show different resistivity value at resting conditions. For instance, the conductivity of the non-electroporated derma is close to 0.2 S/m and the cartilage is 0.16 S/m, whereas fat is close to 0.012 S/m. The electric field distribution can be affected by the variation in the tissue electrical parameters, and hence the desired outcome could not be obtained in all the treated areas.

Typically, a homogeneous model of the tissue is used and its electric field distribution is studied. In this research, the authors show by numerical simulations and phantom experiments, the effect of the presence of inhomogeneous area between the needles used to apply electric field. The phantoms are built using potato that becomes dark if electroporated, and a Tissue-Mimic-Material (TMM), where the resistivity can be suitably designed. For this purpose, a pair of needles, with 2 cm gap was used to apply electric field. Both the numerical model and the phantom include a parallelepiped of homogeneous material with needles and a hole with diameter 9 mm, filled with materials with different resistivities. The hole in the middle, between the needles, simulates the inhomogeneity. This model can show the variation in the electric field when tissue inhomogeneities occur.

The numerical model computes the electric field by means of the Laplace equation solving a static conduction problem. The results obtained with potato phantom and numerical models were compared. The results illustrate the variation in the electric field at different regions. Eventually, these results could be extended to clinical practice.

II. Materials and Methods

A. The numerical model

The model for Finite Element Analysis (FEA) is shown in Fig. 1. It is a parallelepiped (40×30×10.5mm) with a cylinder. The cylinder has a diameter of 9 mm. This way the volume is divided into two sub-volumes that can be filled with material with different electrical characteristics. The electric field is generated between two cylindrical elecrodes 10 mm long, with diameter 0.5 mm, separated by a distance d =20 mm. The two volumes are made of materials characterized by different electrical resistivities, ρ_i (E), one with the electrical resistivity of the potato tuber and the second made of a gel for which the electrical resistance can be designed suitably. The two needle are positioned in the parallelepiped outside from the cylinder. A voltage of 2000 V is applied between the needles.

The electric fields in the different volumes of the model are computed solving a static conduction problem by means of Finite Element analysis. In particular, the Laplace equation in electric potential V, was solved as in [12–18] using a commercial software based on Finite Elements (Flux 3D, Cedrat):

$$\nabla \cdot \sigma(E) \nabla V = 0 \tag{1}$$

imposing $\partial V/\partial n = 0$ on external boundary and a constant electric potentials $V_1 = -V/2$ and $V_2 = +V/2$, respectively to each electrode's surfaces (Dirichlet conditions) [13,15–17].

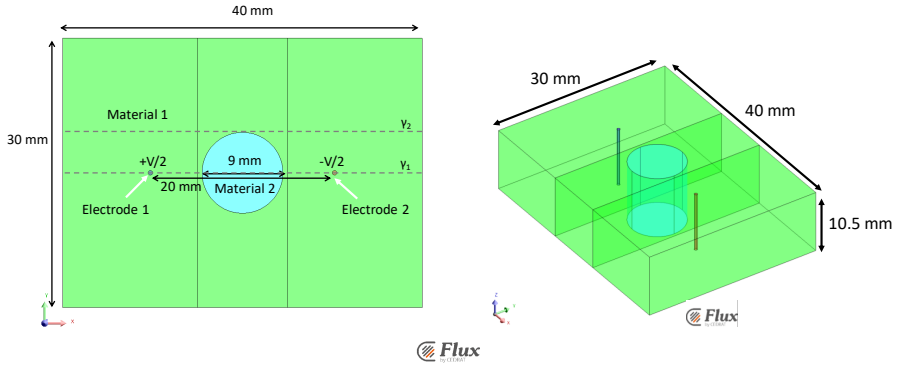

Fig. 1. The geometry used in FEA

In (1) the conductivity, σ [S/m], could be constant or dependent on the electric field intensity, E [V/m]. In particular, a model to describe the potato conductivity dependent on electric field intensity is [19]:

$$\sigma(E) = \left(\sigma_0 + \frac{\sigma_1 - \sigma_0}{2}(1 + \tanh(k_v(E - E_{th})))\right) \quad (2)$$

The typical range for conductivity σ is between 0.15 (for σ_0) and 1 S/m (for σ_1). These values were measured for 'electropored' and 'not electropored' potato tissue, respectively. E_{th} and k_v were evaluated fitting experimental data as in [18].

The simulations were performed for six different values of gel conductivity between 0.15 and 10 S/m. One simulation was performed considering the central cylinder made of potato tissue.

B. Gel phantom preparation

The gel phantoms were prepared according to a procedure based on the one proposed by Mobashsher [21] and adapted from the original in [18,20]. The receipt in [21] is suitable for the preparation of low-cost tissue-mimicking materials (e.g. spinal cord, SC and dura, D), whereas in [18,20] it has been modified in order to tune the tissue resistivity at different values. Gelatine (bought at local market), deionized water, Agar (Meat Liver Agar Sigma-Aldrich 46379), corn starch (bought at local market), glycerine and sodium chloride (NaCl) were used as received. The list and amount of ingredients is reported in Table 1 [20, 21].

Table 1: amount of ingredients for gel preparation

	corn starch	**glycerin**	**Agar**	**gelatin**	**NaCl**
D2	25 g	2 g	1 g	--	1 g
SC1	30 g	0.9 g	--	0.6 g	0.3 g
SC2	30 g	0.9 g	--	0.6 g	0.6 g
SC3	30 g	0.9 g	--	0.6 g	0.15 g

The tissue-mimic material is prepared [20] using the following 4 steps:

(i) mixing of deionized water and corn starch, while stirring vigorously;

(ii) preparation of the gelatin or agar thick mixture by heating it at 90°C with 50 ml of

deionized water and NaCl for 30 seconds;

(iii) mixing the above two by heating for 15 seconds, each time, with manual stirring until the whole mixture turns semi-solid;

(iv) The semi-solid material is cast into boxes or samples with suitable sizes for the experiments.

C. The evaluation of the material resistivity

The electrical resistivity, ρ, of the gel phantoms and potato tissue was evaluated experimentally casting the material in a suitable multi-box with rectangular section (11 x 9 mm, thickness 11.3 mm). In particular each box is a parallelepiped with size (11 x 9 x 11.3 mm). The electrical properties were evaluated applying to two parallel side of the parallelepiped (the ones 11 mm long) a voltage by means of a suitable electrode. The electrode was formed by two plates with rectangular geometry and with the side10 mm long and distant L= 7.5 mm (width 10 mm) as shown in Fig. 2. The 8 voltage pulses were applied to the electrode plates by means of a voltage pulse generator (e.g. EPS01 manufactured by Igea, Carpi, Italy) and the corresponding current is measured. From voltage and current samples the resistance was computed as in [22] and the corresponding conductivity ($\sigma=\rho^{-1}$, ρ resistivity) was computed by means of Ohm's law and the model for resistance, R, of a parallelepiped sample with length L (7.5 mm) and section A (10 x 11.3 mm) as in [22]:

$$\sigma = \frac{1}{R}\frac{L}{A} \tag{3}$$

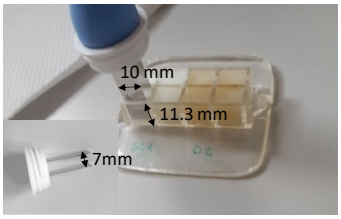

Fig. 2 Set up for electrical conductivity measurements [22]

The described experimental method was used to evaluate the resistivity for both gels and potato tissue. For homogeneous gels prepared following Table 1 and cast in the multi-box the voltage pulses applied has amplitude both 100 V (E=130 V/cm) and 760 V (E=1000 V/cm)). For each gel, two samples was prepared and treated with voltage pulses. For potato, 8 sequences of 8 voltage pulses were applied to 8 pairs of samples. The amplitude of the applied voltage pulses and the corresponding electric field in [V/cm] is in Table 2. For each values of applied voltage the resistivity, ρ, and conductivity, σ, were computed as well as their standard deviation.

D. The Electroporation protocol

Unipolar square voltage pulses, generated using BTX ECM 830 electroporator (Genetronics Inc., San Diego, CA), were applied at the needles. The frequency of the 8 pulses is 1 Hz with pulse length 100 μs. The pulse parameters are chosen as in [8,13].

The voltage pulses were applied by means of needle electrodes to samples similar to the

one in Fig. 1 where the cylinder was casted with one of the gels in Table 1. Two samples for each of the 4 gels in Table 1 were prepared. The external material was potato tissue with electrical characteristics in Table 2.

III. Results and Discussion

A. The material resistivity

Table 2 reports the resistivity of potato tissue at different electric field value and Fig. 3 the color of potato piece 24h after the voltage pulse applications. From the data in Table 2, it appears that the potato resistivity decreases if the applied electric field increases. When the electric field varies from 130 V/cm to 267 V/cm, the resistivity variation is larger than 20%, whereas for stronger electric fields, it is close to 5%.

Table 2: potato sample resistivity and conductivity at different electric field values

Voltage [V]	E[V/cm]	ρ[Ωm]	std(ρ)[Ωm]	σ[S/m]	std(σ)[S/m]
0	0	6.50	1.21	0.16	0.03
100	133	6.50	1.21	0.16	0.03
150	200	4.08	1.29	0.27	0.09
200	267	3.19	0.49	0.32	0.05
400	533	1.30	0.03	0.77	0.02
500	667	1.37	0.06	0.73	0.03
600	800	1.31	0.04	0.76	0.02
700	933	1.30	0.10	0.77	0.06
800	1067	1.38	0.11	0.73	0.06

From the potato data, the parameters of the equation (2) were evaluated by means of a Minimum least Square fitting of experimental data.

Table 3 shows the resistivity and conductivity and their standard deviation for gels in Table 1 evaluated as previously described, but applying 8 rectangular voltage pulses at 100V and at 700V. The data in Table 3 are the average between the values found at 100 v and the one at 700 V, since the values are similar. Each type of measurement was repeated at least 2 times.

Table3: Gel resistivity and conductivity

sample	ρ[Ωm]	std(ρ)[Ωm]	σ[S/m]	std(σ)[S/m]
SC3	4.16	0.30	0.24	0.02
SC1	2.03	0.08	0.49	0.02
SC2	1.35	0.11	0.75	0.06
D2	0.61	0.05	1.68	0.13

Table 2 reports the resistivity for potato tuber evaluated by means of equation (3) varying the applied voltage averaging at least 2 values. From these values of resistivity, the conductivity values for electroporated (ρ_1 = 1.38 Ωm, σ_1 = 0.73 S/m) and not-

electroporated (ρ_0 = 6.5 Ωm, σ_0 = 0.16 S/m) tissue used in the equation (2) were computed. Moreover, by means of Minimum least Square fitting, E_{th}, the threshold was found and it is equal to 315 V/cm. This value is between the field values 267 and 533 V/cm, where the color change of potato cubes occurs as shown in Fig. 3.

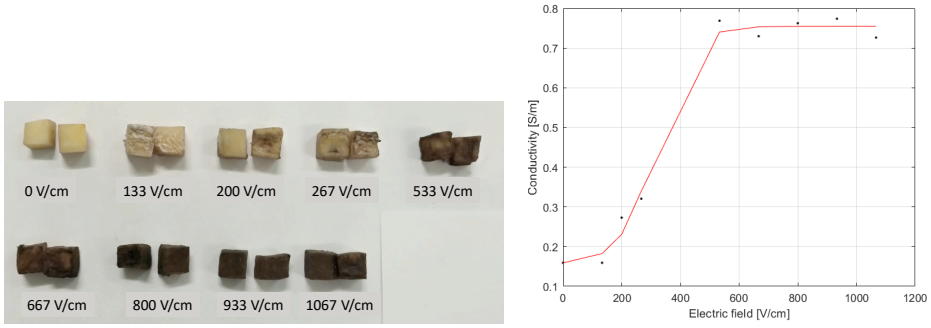

(a) (b)

Fig. 3. (a) Potato cubes treated with voltage pulses with different amplitude; (b) fit of experimental data

The potato cubes treated with an electric field larger than 533V/cm are dark and it is evident that the tuber is electroporated. The value at which the tuber start to be dark an this value is coherent to the ones in literature [9], [10]. Finally, the coefficient k_v results equal to 0.008622 cm/V. Increasing the electric field intensity the potatoes show a more intense dark color.

B. Simulations results

Fig. 4 shows the line levels of electric field evaluated on the xy surface of the model in Fig. 1 when the cylinder has the electrical properties of the potato tissue and the electric field and the conductivity evaluated along the lines γ_1 and γ_2 in Fig. 1.

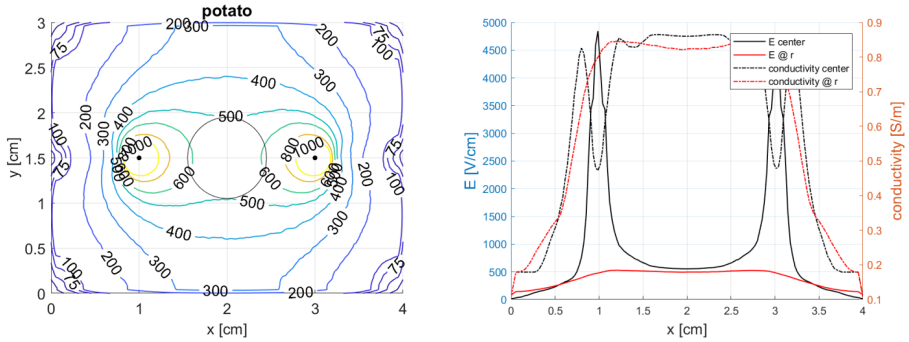

(a) (b)

Fig. 4. (a) The electric field equi-level lines and (b) the electric field and conductivity along the lines γ_1 and γ_2 in Fig. 1 considering the cylinder made of potato tissue

Fig. 5 illustrates the simulation results considering different values for the cylinder conductivity (from 0.15 to 10 s/m). It shows the electric field and conductivity value as a function of the x-coordinate sampled along the lines γ_1 and γ_2 in Fig. 1.

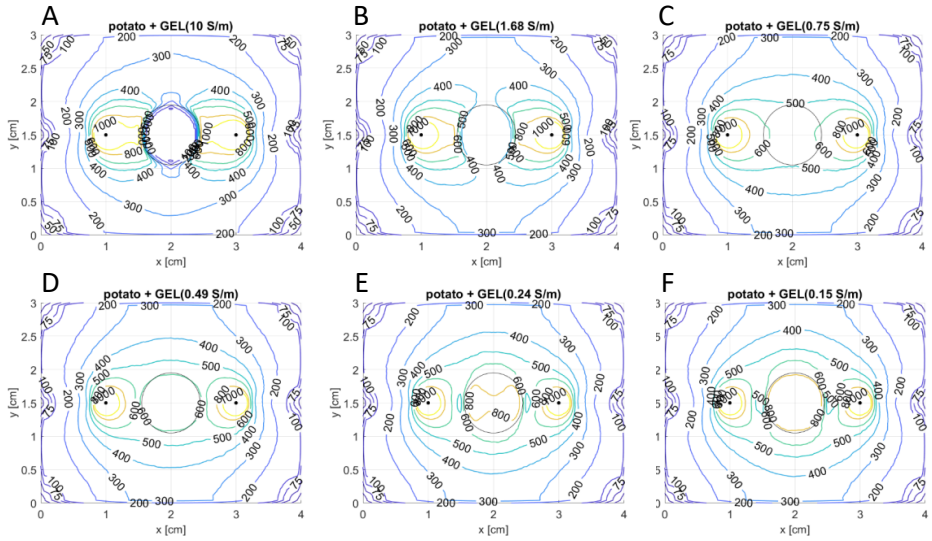

Fig. 5. Electric field equi-lines for different values of the conductivity of the cylinder. A: σ=10 S/m; B: σ=1.68 S/m; C: σ=0.75 S/m; D: σ=0.49 S/m; E: σ=0.24 S/m; F: σ=0.15 S/m.

From Figs. 4 and 5 the different distributions of the electric field appears in the model surface when the different value for cylinder conductivity are considered. Then if the tissue treated by means voltage pulses is not homogenous in terms of conductivity, the treated area could not be affected by the electric field strength able to electropore the cell membranes.

For instance, consider the cases A and B in Fig. 6, the electric field in the cylinder (conductivity of 10 S/m and 1.68 S/m, respectively). In these cases the electric field is lower than 500 V/cm that is the electric field found in the cylinder of the homogeneous model (data in Fig. 4(b)); whereas if the conductivity in the cylinder is lower the electric field is higher than 500 V/cm.

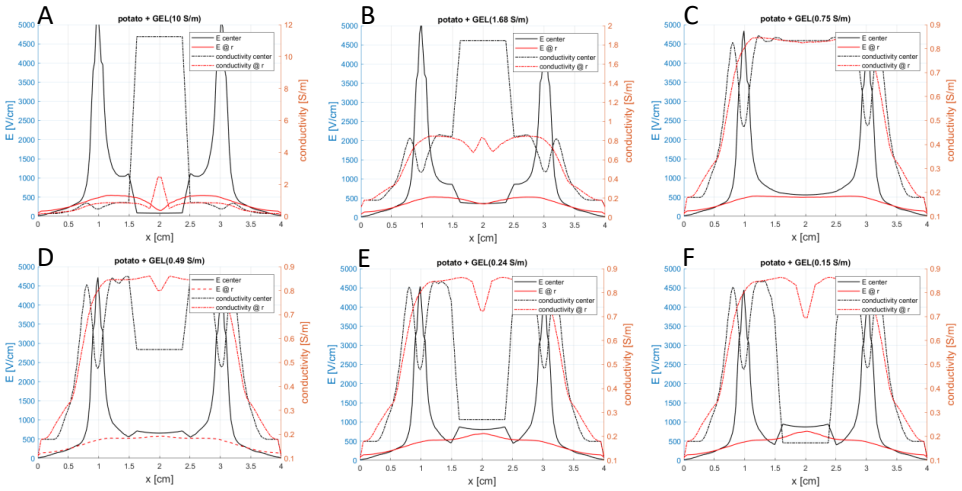

Fig. 6. Electric field and conductivity along the lines γ_1 and γ_2 in Fig. 1 evaluated for different values of the conductivity of the cylinder. A: σ=10 S/m; B: σ=1.68 S/m; C: σ=0.75 S/m; D: σ=0.49 S/m; E: σ=0.24 S/m; F: σ=0.15 S/m.

C. Experimental results

Fig. 7 shows the potato samples 24 h after the voltage pulses. The electric field distribution was similar to the one reported in Fig. 5. In this case the dark area correspond to the 500V/cm electric field level line in Fig. 5.

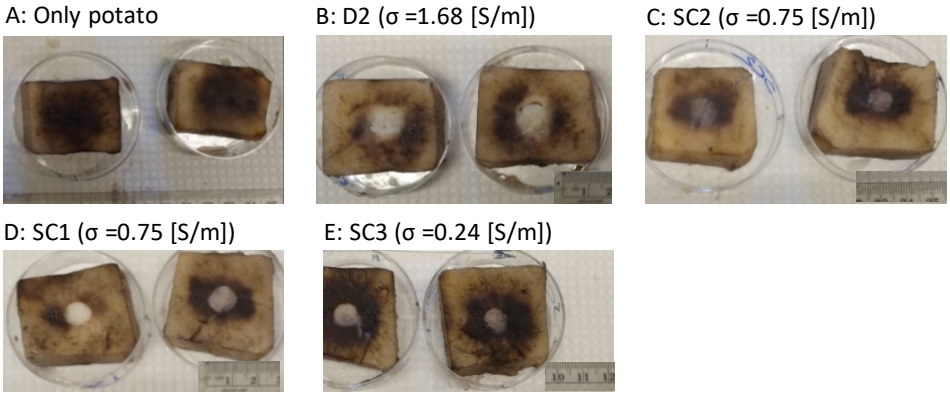

Fig. 7. Experimental results on potato phantom: field and conductivity along the line γ_1 andγ_2 in Fig. 1 evaluated for different value of the conductivity of the cylinder. A: only potato and potato with gel with different conductivity B: σ=1.68 S/m (D2); C: σ=0.75 S/m (SC2); D: σ=0.49 S/m (SC1) and E: σ=0.24 S/m (SC3).

IV. CONCLUSIONS

- Cancer tissue inhomogeneity could be modeled using potato tissue and gel models.
- The higher the electric field, the darker is the tissue color.

- The proposed model enables to visualize how the inhomogeneity in electric conductivity affect the electric field distribution in electroporation condition.

ACKNOWLEDGMENT

Authors (Mittal and Sundararajan) gratefully acknowledges the partial funding support by the Purdue Polytechnic Institute, West Lafayette, under Dean's award GRA – FY16.

REFERENCES

[1] L.M. Mir, Therapeutic perspectives of in vivo cell electropermeabilization, Bioelectrochemistry. 53 (2001) 1–10. doi:10.1016/S0302-4598(00)00112-4.

[2] L.M. Mir, S. Orlowski, Mechanisms of electrochemotherapy, Advanced Drug Delivery Reviews. 35 (1999) 107–118. doi:10.1016/S0169-409X(98)00066-0.

[3] R. Sundararajan, Electroporation-Based Therapies for Cancer: From Basics to Clinical Applications, Woodhead Publishing Limited, 2014. http://books.google.it/books?id=28dQXwAACAAJ.

[4] IGEA, (n.d.). http://www.igeamedical.com/ (accessed April 15, 2014).

[5] M. Marty, G. Sersa, J.R. Garbay, J. Gehl, C.G. Collins, M. Snoj, V. Billard, P.F. Geertsen, J.O. Larkin, D. Miklavcic, I. Pavlovic, S.M. Paulin-Kosir, M. Cemazar, N. Morsli, D.M. Soden, Z. Rudolf, C. Robert, G.C. O'Sullivan, L.M. Mir, Electrochemotherapy – An easy, highly effective and safe treatment of cutaneous and subcutaneous metastases: Results of ESOPE (European Standard Operating Procedures of Electrochemotherapy) study, European Journal of Cancer Supplements. 4 (2006) 3–13. doi:10.1016/j.ejcsup.2006.08.002.

[6] L.M. Mir, J. Gehl, G. Sersa, C.G. Collins, J.-R. Garbay, V. Billard, P.F. Geertsen, Z. Rudolf, G.C. O'Sullivan, M. Marty, Standard operating procedures of the electrochemotherapy: Instructions for the use of bleomycin or cisplatin administered either systemically or locally and electric pulses delivered by the CliniporatorTM by means of invasive or non-invasive electrodes, EJC Supplements. 4 (2006) 14–25.

[7] L.G. Campana, F. Dughiero, M. Forzan, C.R. Rossi, E. Sieni, A prototype of a flexible grid electrode to treat widespread superficial tumors by means of Electrochemotherapy, Radiol Oncol. 50 (2016) 49–57. doi:10.1515/raon-2016-0013.

[8] M. Castiello, F. Dughiero, F. Scandola, E. Sieni, L.G. Campana, C.R. Rossi, M.D. Mattei, A. Pellati, A. Ongaro, A new grid electrode for electrochemotherapy treatment of large skin tumors, Dielectrics and Electrical Insulation, IEEE Transactions On. 21 (2014) 1424–1432. doi:10.1109/TDEI.2014.6832291.

[9] F. Dughiero, E. Sieni, C.R. Rossi, L.G. Campana, APPLICATORE PER ELETTROPORAZIONE, VR2013A000184, 2015.

[10] M. Rebersek, T. Cufer, M. Cemazar, S. Kranjc, G. Sersa, Electrochemotherapy with cisplatin of cutaneous tumor lesions in breast cancer, Anticancer Drugs. 15 (2004) 593–597.

[11] G. Sersa, T. Cufer, S.M. Paulin, M. Cemazar, M. Snoj, Electrochemotherapy of chest wall breast cancer recurrence, Cancer Treat. Rev. 38 (2012) 379–386. doi:10.1016/j.ctrv.2011.07.006.

[12] A. Ongaro, L.G. Campana, M. De Mattei, F. Dughiero, M. Forzan, A. Pellati, E. Sieni, C.R. Rossi, Effect of Electrode Distance in Electrochemotherapy: From Numerical Model to in Vitro Tests, in: T. Jarm, P. Kramar (Eds.), 1st World Congress on Electroporation and Pulsed Electric Fields in Biology, Medicine and Food & Environmental Technologies, Springer Singapore, 2016: pp. 167–170. http://dx.doi.org/10.1007/978-981-287-817-5_37.

[13] A. Ongaro, L.G. Campana, M. De Mattei, F. Dughiero, M. Forzan, A. Pellati, C.R. Rossi, E. Sieni, Evaluation of the Electroporation Efficiency of a Grid Electrode for Electrochemotherapy: From Numerical Model to In Vitro Tests, Technology in Cancer Research & Treatment. 15 (2016) 296–307. doi:10.1177/1533034615582350.

[14] S. Corovic, I. Lackovic, P. Sustaric, T. Sustar, T. Rodic, D. Miklavcic, Modeling of electric field distribution in tissues during electroporation, BioMedical Engineering OnLine. 12 (2013) 16.

[15] N. Pavselj, D. Miklavcic, Numerical Models of Skin Electropermeabilization Taking Into Account Conductivity Changes and the Presence of Local Transport Regions, Plasma Science, IEEE Transactions on DOI - 10.1109/TPS.2008.928715. 36 (2008) 1650–1658.

[16] L.G. Campana, P. Di Barba, F. Dughiero, C.R. Rossi, E. Sieni, Optimal Needle Positioning for Electrochemotherapy: A Constrained Multiobjective Strategy, IEEE Transactions on Magnetics. 49 (2013) 2141–2144. doi:10.1109/TMAG.2013.2241031.

[17] S. Corovic, A. Zupanic, D. Miklavcic, Numerical Modeling and Optimization of Electric Field Distribution in Subcutaneous Tumor Treated With Electrochemotherapy Using Needle Electrodes, Plasma Science, IEEE Transactions on DOI - 10.1109/TPS.2008.2000996. 36 (2008) 1665–1672.

[18] A. Bernardis, M. Bullo, L.G. Campana, P. Di Barba, F. Dughiero, M. Forzan, M.E. Mognaschi, P. Sgarbossa, E. Sieni, Electric field computation and measurements in the electroporation of inhomogeneous samples, Open Physics. 15 (2017). doi:10.1515/phys-2017-0092.

[19] M. Breton, F. Buret, L. Krahenbuhl, M. Leguebe, L.M. Mir, R. Perrussel, C. Poignard, R. Scorretti, D. Voyer, Non-Linear Steady-State Electrical Current Modeling for the Electropermeabilization of Biological Tissue, IEEE Transactions on Magnetics. 51 (2015) 1–4. doi:10.1109/TMAG.2014.2351836.

[20] L.G. Campana, Di Barba Paolo, M. E. Mognaschi, M. Bullo, F. Dughiero, M. Forzan, P. Sgarbossa, E. Spessot, E. Sieni, Electrical resistance in inhomogeneous samples during electroporation, in: Proc SMACD, 2017.

[21] A.T. Mobashsher, A.M. Abbosh, Three-Dimensional Human Head Phantom With Realistic Electrical Properties and Anatomy, IEEE Antennas and Wireless Propagation Letters. 13 (2014) 1401–1404. doi:10.1109/LAWP.2014.2340409.

[22] L.G. Campana, M. Cesari, F. Dughiero, M. Forzan, M. Rastrelli, C.R. Rossi, E. Sieni, A.L. Tosi, Electrical resistance of human soft tissue sarcomas: an ex vivo study on surgical specimens, Medical & Biological Engineering & Computing. 54 (2016) 773–787. doi:10.1007/s11517-015-1368-6.